

## CROSSTALK ANALYSIS OF SUPRIME-CAM FDCCDS USING COSMIC RAYS IN DARK FRAMES

MASAFUMI YAGI

Optical and Infrared Astronomy Division, National Astronomical Observatory of Japan, Mitaka, Tokyo, 181-8588, Japan  
YAGI.Masafumi@nao.ac.jp  
Draft version May 25, 2022

### ABSTRACT

We analyzed the crosstalks in the new full depleted CCDs in the Subaru Prime Focus Camera(Suprime-Cam). The effect is evaluated quantitatively using cosmic rays in dark frames. The crosstalk is well approximated by a linear correlation and the coefficient is  $\sim 10^{-4}$ . The coefficients are not significantly different among the 10 CCDs. We also find that the crosstalk appears not only in the corresponding pixels but also in the next pixel but one. No crosstalk is detected in Suprime-Cam among different CCDs. Based on the analysis, the correction procedure for the crosstalk is presented, and the application to the data is demonstrated.

*Subject headings:* Data Analysis and Techniques – Astronomical Instrumentation

### 1. INTRODUCTION

Multi-channel CCD often suffers from a crosstalk phenomenon between readout channels. There are several user documents describing the crosstalk<sup>1,2,3,4</sup> and some observatories prepare data to correct this crosstalk<sup>5</sup>. Freyhammer et al. (2001) estimated the effect in DFOSC and FORS1 at the ESO VLT. The studies for Advanced Camera for Surveys (ACS) in Hubble Space Telescope (HST) is also available (Giavalisco 2004a,b; Suchkov et al. 2010; Suchkov & Baggett 2012).

Since the replacement of the CCDs in July 2008 with full depleted back illuminated CCDs (FDCCD; Kamata et al. 2008), the data of Subaru Prime Focus Camera (Suprime-Cam; Miyazaki et al. 2002) show crosstalk signatures in a CCD. The effect is easily recognized in narrowband data with low sky background (Figure 1). As one of the crosstalk dimming regions (shadows) has the same spatial parity as the source, it obtains a higher signal-to-noise ratio(S/N) after coadding (Figure 2), and causes a problem even in a deep field study.

In this paper, we investigated the crosstalk effect in Suprime-Cam in order to remedy this problem. We adopted a method using cosmic rays in dark frames, and present a recipe to remedy the crosstalk effects.

### 2. MODELS AND METHOD

#### 2.1. *Suprime-Cam*

Suprime-Cam is equipped with 10 FDCCDs, and each FC-CCD is read out from 4 channels. In this paper, we call the channels chA, chB, chC, and chD along the x-axis of the output FITS file for simplicity. The data from each channel consist of  $512 \times 4177$  CCD pixels,  $8 \times 4177$  pixels of the prescan region of serial read and  $48 \times 4177$  pixels of the overscan region of serial read, followed by  $(8+512+48) \times 48$  pixels overscan of parallel read. The FITS data have an additional  $(8+512+48) \times 48$  pixels in the prescan region, but it should not be used for the analysis (Figure 3). The 10 CCDs are arranged in 2 rows of 5 CCDs each<sup>6</sup>. The CCDs in the upper row (detector ID=0,1,2,6,7) are

read from the top edge ( $y=4177$ ), and those in the lower row (detector ID=3,4,5,8,9) are read from the bottom edge ( $y=1$ ).

When a CCD is read out, the charges stored in each pixel are converted to voltage at on-chip amplifiers(on-chip amps) at 4 channels. The conversion factor of the on-chip amps has  $\sim 15\%$  difference. Suprime-Cam is equipped with 40 preamplifiers(preamps) arranged in 10 quad-channel preamp boards around the camera dewar. One preamp board handles signals from a CCD. The gain of the preamp is 3 (Nakaya et al. 2008) and the difference among the 40 preamps is  $\sim 1\%$  (Nakaya, H. 2012; private communication). The signals are then put into the signal board (SIG) and a correlated double sampling is performed (Nakaya et al. 2012). Suprime-Cam has 5 SIG boards, and one SIG board has 8 channels. The signals from CCD0 and CCD1 are into the first SIG board, those from CCD2 and CCD3 are into the next, and so on. The signal is then converted into a digital value. The analog-to-digital conversion factor is configured to be 1 (Nakaya et al. 2008), but slightly differs at each channel by  $\sim 5\%$ . The total gain of the Suprime-Cam data is the product of the three gains of the components; the gain of the analog-to-digital converter (ADC) in the SIG at each channel( $g_1$ ), the gain of the preamp ( $g_2$ ), and the gain of the on-chip amp at each channel( $g_3$ ). A schematic figure is shown as Figure 4.

The charges in CCDs are read out and converted to the digital data simultaneously in 40 channels. For example, when  $(x,y)$  of CCD0 is read,  $(1024-x,y)$ ,  $(1024+x,y)$ , and  $(2048-x,y)$  of CCDs in the upper row and  $(x,4178-y)$ ,  $(1024-x,4178-y)$ ,  $(1024+x,4178-y)$ , and  $(2048-x,4178-y)$  of CCDs in the lower row are read at the same time.

#### 2.2. *Crosstalk in Suprime-Cam*

The apparent crosstalk appears as follows. When a bright object is observed at  $(x,y)$  in chA, shadows appear at three symmetric positions of saturated stars; at  $(1024-x,y)$  in chB, at  $(1024+x,y)$  in chC, and at  $(2048-x,y)$  in chD, which are read out at the same time. Currently, the crosstalk in the same CCD, the

<sup>1</sup> [http://www.noao.edu/kpno/mosaic/manual/mosa\\_2.html](http://www.noao.edu/kpno/mosaic/manual/mosa_2.html)

<sup>2</sup> <http://www.astronomy.ohio-state.edu/MDM/MDM4K/>

<sup>3</sup> [http://www.stsci.edu/hst/acs/performance/anomalies/zoo\\_xtalk.html](http://www.stsci.edu/hst/acs/performance/anomalies/zoo_xtalk.html)

<sup>4</sup> <http://www.ast.cam.ac.uk/iao/research/vdfs/docs/reports/sv/>

<sup>5</sup> <http://www.noao.edu/noao/mosaic/calibs.html>

<sup>6</sup> <http://www.naoj.org/Observing/Instruments/SCam/ccd.html>

pixels read at the same time show an apparent crosstalk. The possible crosstalk across the CCDs, and effect on the adjacent pixels in the same CCD are examined later.

In the three shadows corresponding to  $(x,y)$ ,  $(1024-x,y)$  and  $(2048-x,y)$ , can be removed by dithering, as their position at the sky changes when the telescope pointing is changed. However, the movement of the shadow at  $(1024+x,y)$  is the same as the object at  $(x,y)$ , and the shadow gains S/N when we coadd the dithered images (Figure 2 right), if the shadow is larger than the slight differential shift by the optical distortion at the dithered pointing. The existence of the shadow of the same parity is different from quadrantic readout devices, such as ACS/HST and FORS1/VLT. As investigated in a later section, the shadow of the same parity causes problems in deep field imaging in broadband, though the effect cannot be detected in a single exposure.

### 2.3. Signal variables

If the crosstalk occurs around the input of the on-chip amps, the effect would correlate with the raw charge  $v \times (g_1 \times g_2 \times g_3)$ , where  $v$  is the value in output FITS file after the bias subtraction. If the crosstalk occurs between output of the on-chip amps and input of the preamps, the effect would correlate with  $v \times (g_1 \times g_2)$ , and if between output of preamps and input of ADC, the effect would correlate with  $v \times g_1$ .

We estimated the relative value of the total gain  $g_1 \times g_2 \times g_3$  and the relative gain of SIG+preamps,  $g_1 \times g_2$ , and listed them in Tables 2 and 3. The detail of the estimation is described in the Appendix. Though we do not have  $v_2$  nor  $v_3$  data, the difference of  $g_1$  and  $g_1 \times g_2$  is small, since the difference of  $g_2$  is only  $\sim 1\%$  among the 40 preamps.

Using the relative gain values, we obtain three different signal values;  $v_1 = v$ ,  $v_2 = v \times (g_1 \times g_2)$ , and  $v_3 = v \times (g_1 \times g_2 \times g_3)$ .  $v_1$  is the count in FITS file in analog-to-digital unit (ADU),  $v_2$  is proportional to the voltage between the on-chip amps and the SIG, and  $v_3$  is proportional to the charge in a pixel.

## 3. ANALYSIS

### 3.1. Method

We can evaluate the crosstalk by taking the correlation between pixels in channel X and channel Y, when the pixel in X has a large count and the pixel in Y has a smaller count. A linear trend of crosstalk effect was reported by previous studies on other CCDs (e.g., Freyhammer et al. 2001; Suchkov et al. 2010). Under the assumption that the crosstalk is linear to the source, the strength of the crosstalk is measured by the coefficient of proportionality. The coefficient of other instruments are about  $\sim 10^{-4}$ ; ACS/HST has  $-0.6..-2.3 \times 10^{-4}$  (Suchkov & Baggett 2012) and FORS1/VLT has  $-2.3..-2.5 \times 10^{-4}$  (Freyhammer et al. 2001). It should be noted that the readout count suffers from the quantization error, and the difference smaller than 1 ADU in a certain pixel is buried in the noise. Since the maximum output is  $2^{16} - 1 = 65535$  ADU in Suprime-Cam, the crosstalk coefficient is meaningful when its absolute value is larger than  $1/(2^{16} - 1) \sim 1.5 \times 10^{-5}$ .

There are several types of data for measuring the correlation. Freyhammer et al. (2001) used a calibration lamp with a mask on the focal plane and a night sky with standard stars. Suchkov

et al. (2010) used dark frames and sky frames. In this work, we only use dark frames and cosmic rays<sup>7</sup> to minimize the error from flat fielding and the background level estimation. The small spatial size of the high count pixels in cosmic rays, even smaller than the point spread function (PSF), enables us to examine a possible spatial extent of the crosstalk shadow over a pixel. Moreover, the FDCCD of Suprime-Cam and the Subaru Telescope have several advantages for using cosmic rays in dark frames. Thanks to the thickness of the FDCCD ( $250\mu\text{m}$ ) and the high altitude of the Subaru Telescope, Suprime-Cam receives a relatively large number of cosmic rays. The dark current is very low; less than 0.6 ADU per hour, and the readout noise is also low; 2-2.5 ADU in rms (Kamata et al. 2008). The acquisition of dark frames does not require either a special instrument setting such as a mask, nor a telescope time at night. We can take a dark frames in a daytime if we can keep the instrument in the dark. On the other hand, the drawback of this method is that it is not easy to obtain enough data of high-value count pixels. For example, we could not investigate the behavior near the full-well region in this study, because of the lack of such data.

### 3.2. Data

We used all dark frames with EXPTIME  $\geq 120$  seconds taken between 2008/12/03 and 2011/07/02 (UT); after the fix of the linearity problem, and before the hardware incident of the Subaru. The data are retrieved from MASTARS<sup>8</sup> and the SMOKA<sup>9</sup> archives. The used frames are summarized in Table 1.

Bias is first subtracted using the median of 48 pixels in the serial overscan region at each y. The bias level has a  $\sim 2$  ADU waving pattern in x direction as shown in Figure 6. The pattern is common in all the CCDs, in all the channels, and in all the exposures as far as we examined in the dark frames. This pattern is corrected using the data in the parallel overscan region. The median of the parallel overscan after the subtraction of the serial overscan of the parallel overscan reflects the pattern, and it is subtracted from the data in each frame. Finally, the dark is subtracted, and we call the value after the mean dark subtraction as  $v_1$ , hereafter.

The dark level is estimated by averaging the count in a channel avoiding the pixels which are hit by cosmic rays or are affected by the crosstalk because of a high count in other channels. The mean dark count is various in different CCDs and channels. The typical count of dark is  $(0.16 \pm 0.09)$  ADU for 300 second exposure ( $(5 \pm 3) \times 10^{-4}$  ADU  $\text{s}^{-1}$ ), and the rms is  $(2.2 \pm 0.2)$  ADU. The rms includes readout noise and the error of bias/overscan subtraction. As the total gain of Suprime-Cam is about 3–4 electron  $\text{ADU}^{-1}$ , the mean dark count is less than 1 electron.

In the bias and the dark corrected dark images, high count pixels are picked up and then corresponding pixels in other 3 channels in the same CCD are checked. We arbitrarily adopted the threshold of the ‘‘high’’ count as 300 ADUs in  $v_1$ . Total 1277705 pixels are marked as a high count pixel in the 370 frames. The count of the three corresponding pixels to the high count pixel is cataloged. When taking the correlation of  $v_1(X)$  as the high count and  $v_1(Y)$  as the affected count,  $v_1(Y)$  should be corrected the dark count, but  $v_1(X)$  should not, since the

<sup>7</sup> We do not distinguish cosmic rays and hot pixels and simply call them ‘‘cosmic rays.’’

<sup>8</sup> <http://www.mastars.nao.ac.jp/>

<sup>9</sup> <http://smoka.nao.ac.jp/>

dark count would also contribute to the crosstalk. However, as we take the  $v_1(X) > 300$  as the high count in following analysis, the effect of the dark subtraction of 0.16 ADU makes 0.05% error in the coefficient. The error is negligible, as we estimate the coefficients with 3 significant figures. For simplicity, we used the bias and the dark subtracted value for  $v_1(X)$  instead of the bias subtracted value.

### 3.3. The fundamental variable

In Fig. 7 an example of the correlation is shown. The data are CCD0 and a high pixel is at chB and the checked the corresponding pixel in chD. Apparent linear correlation is recognized. The result shows that the shadow appears even in the dark data with negligible ( $< 1ADU$ ) background charges. It suggests that the crosstalk phenomenon in Suprime-Cam should be a slight shift of the zero level. This assumption is consistent with the result by Gialvalisco (2004a) that the effect is additive and not multiplicative. We can therefore expect that an additive correction established with these negligible background data is also valid for the object images with sky backgrounds.

We then multiply two kinds of relative gain to  $v_1$ . One is the value multiplied by the SIG+preamp gain in Table 3. It represents the voltage between the output of the on-chip amp and the input of SIG. We call it  $v_2$ . The other is the value multiplied by the total gain in Table 2, which is proportional to the photo-charges. We call it  $v_3$ . The question is which is the fundamental variable,  $v_1$ ,  $v_2$  or  $v_3$ . As the gains are different among channels, the behavior of the three variables is different. A clue is  $\sim 14\%$  change of gain of the on-chip amp of chA of CCD9 in 2010/10. If crosstalk depends on photo-charges ( $v_3$ ), the coefficient of the crosstalk should change if the gain of on-chip amp ( $g_3$ ) changes. If crosstalk does not depend on the gain, the coefficient should remain the same.

We calculated the regression line using the data before the change of the gain, and tested whether the data after the change follow the same regression line. For the regression, we estimated the distribution of  $v(\text{other})$ , especially the fraction of outliers. The distribution of the pixel values which are not affected by the high count pixels is well approximated by Gaussian in  $-5\sigma < v < 5\sigma$ , with several ( $\sim 1.1 \times 10^{-4}$ ) outliers on the positive side. The fraction is much larger than the expected fraction of  $\leq 5\sigma$  in Gaussian,  $5.7 \times 10^{-7}$ , and possibly due to weak radiation events. If we exclude  $\geq 5\sigma$  data in normal distribution, the expected reduced  $\chi^2$  is only  $1.5 \times 10^{-5}$  smaller. Therefore, we neglect the effect of the truncation as  $\chi \leq 5\sigma$ .

We restricted the data that input of high count pixel is in chD and output is in chA in order to exclude the effect of the difference of the coefficients of different combination of the channels discussed in the next section. We adopted chD because it has more high count pixels than chB or chC by chance in our data. From likelihood-ratio test with the critical value of 5%, we obtained the result that the regression of  $v_1$  and  $v_2$  is not significantly different, while the regression of  $v_3$  changes significantly after the change of the gain.

As another check, we plotted the histogram of  $a=v(\text{other};\text{chD})/v(\text{high};\text{chA})$  in  $v(\text{high};\text{chA}) > 15000$  data of  $v_1$  and  $v_3$  in Fig. 8. We can see a shift of the histogram of  $v_3$ , while  $v_1$  remains the same. We therefore conclude that the crosstalk affects  $v_1$  or  $v_2$ , and not  $v_3$ . The result resembles the result by Freyhammer et al. (2001), who noted that ‘‘Changing the gain, e.g. from low to high gain, does not alter the cross-talk

amplitudes, when the cross-talk originates from the CCD itself rather than from the ADCs electronic circuits.’’

The result implies that the crosstalk does not occur inside of the CCD but downstream of output of the on-chip amp. In the following analyses, we do not use  $v_3$ . Whether  $v_2$  is more fundamental than  $v_1$  or not cannot be distinguished by this CCD9 gain analysis. As the difference of  $v_1$  and  $v_2$  is 7% at most as listed in Table 3, the correction of the crosstalk may have a comparable error if the wrong variable is used.

### 3.4. Variation of crosstalk coefficients

We investigated the linear correlation of each CCD of each combination of the channels, because we noticed that some combination of channels have weaker crosstalk signal than others. For example, the chC affected from chB in CCD0 shows weak crosstalk signal as shown in Fig. 9 and Fig. 10.

Ideally, we can estimate all combinations separately by investigating all possible datasets. In our data, however, some combinations do not have enough data at large  $v(\text{high})$  and the error of the estimation of the coefficient is large. We therefore set a working hypothesis and test its validity. The hypothesis is that the coefficient is the same for the same combination in a mirror symmetry. For simplicity, we will call the data where a high count pixel is in chX and the output is chY as crosstalk of XY, and write it as cXY. From the assumption of the mirror symmetry, the combinations are reduced to 4 groups: 4 of cAB-like combinations, which include cAB, cBA, cCD, cDC, 4 of cAC-like ones, 2 of cAD-like ones, and 2 of cBC-like ones. We call the groups as gAB, gAC, gAD, and gBC, respectively. As the small  $v(\text{high})$  data only add the noise, we restricted the fitting range at  $v(\text{high}) > 5000$ . We also tested  $v(\text{high}) > 15000$  but the difference between them is small. The coefficients of the best-fit regressions are shown in Table 5 and 6. The 95% confidence intervals are calculated from likelihood-ratio test. The regression of gAB and gAC have an overlap of the confidence intervals, while other two do not have the overlap.

Then, data of each channel pair are compared with the best-fit function by likelihood-ratio test with the critical value of 5%. One cBC data (CCD5) and two cBC data (CCD0 and CCD5) are significantly different from the best-fit function both in  $v_1$  and  $v_2$ . As the total number of combinations are 120, the expected number of significantly different pairs should follow binomial distribution  $\text{Bi}(120, 0.05)$  in an ideal case. We therefore conclude that the coefficients of the crosstalk are not significantly different in the same symmetry group, and we mix all the chips and the combinations in the same symmetry group hereafter. In future, this hypothesis should be re-examined when more data are available.

As the coefficient of gBC in the same CCD is different from other three, we can assume that the crosstalk may occur around the output of on-chip amp, because the difference of gBC from other three groups exists only inside the CCD package. This implies that  $v_2$  would be the fundamental variable. We therefore use  $v_2$  hereafter.

### 3.5. Profile along x-axis

We checked whether the crosstalk occurs only in the corresponding pixel to the high count pixel. If the crosstalk has a time duration, not only the pixels which were read at the same time but also the pixels which were read later might be affected. For example, if (x,y) in chA has a high count, (1024-(x+ $\Delta x$ ),y) is examined in chB, and also the corresponding pix-

els in chC and chD. We should be careful in the analysis that if  $((x+\Delta x),y)$  in chA is also a high count pixel, the shadow at  $(1024-(x+\Delta x),y)$  would be caused by a normal crosstalk effect from  $((x+\Delta x),y)$ . We therefore set an additional constraint that  $((x+\Delta x),y)$  and corresponding pixels in other three channels should not be high count pixels, i.e.  $v < 300$ . We then found a sign that the confidence intervals of the coefficient are significantly different from 0 at  $\Delta x > 0$ .

For a detailed study, we select the high count pixels which extend only one pixel along the x-axis, and calculate the profile of the crosstalk coefficients along the x-axis. The result is shown in Figure 11, and the coefficients around  $x=0$  are given in Table 7. The errorbars represent the 95% confidence intervals. The readout sequence is toward  $+x$ . The pixel at  $\Delta x=1$  is read out just after the high count pixel is read out, for example. The profile of gAB, gAC, and gAD resemble one another. In  $\Delta x < 0$  region, the coefficient is  $\sim 0$ . At  $\Delta x=0$ , the coefficient is significantly negative. It is the shadow of the crosstalk in Figure 1. Then the coefficient is back to almost 0 at  $x = 1$ , and then *significantly* positive at  $x = 2$ . It resembles a damped oscillation pattern. On the other hand, the profile of gBC shows no significant crosstalk except at  $x=0$ .

### 3.6. Crosstalk across the CCDs

If the crosstalk occurs around SIG, the crosstalk of CCD(2n) and CCD(2n+1) may occur, as they are handled in the same SIG board. The possibility is examined in the same way as in the previous section. We picked up a high count pixel and check the corresponding pixels which are read at the same time in other CCDs. None of the coefficients of the crosstalk across the CCDs is significantly different from 0. If we use all the combinations, the coefficient is  $-0.01 \times 10^{-4}$ , and their 95% confidence interval is  $-0.11 \times 10^{-4} < a < 0.08 \times 10^{-4}$ . The result supports the assumption that the crosstalk would occur around on-chip amp. And the possible small crosstalk across the CCDs is negligible, because the crosstalk effect is buried in the quantization noise if the coefficient is smaller than  $\sim 1.5 \times 10^{-5}$  as discussed in section 3.1.

## 4. CORRECTION OF THE CROSTALK

### 4.1. Procedure

We tried to correct the two significant pixels at  $x = 0$  and  $x = 2$  using the coefficients in Table 7. The recipe is as follows:

1. Prepare an overscan subtracted image.
2. Convert the pixel value ( $v_1$ ) to  $v_2$  using the gain in Table 3.
3. Visit each pixel in the frame.
4. When visiting  $(x,y)$  in chA, calculate the crosstalk effect from  $(1024-x,y)$  as  $\Delta x=0$  and  $(1024-(x+2),y)$  as  $\Delta x=+2$  in chB. The crosstalk from chC and chD are also calculated.
5. Subtract the sum of the effect from the pixel value at  $(x,y)$  in the output frame.

This procedure is based on several assumptions. First, we assumed that the effects from different pixels are additive. The coefficients we use are calculated from isolated signals. We assumed that the crosstalk effect is a simple sum when several

high count pixels are connected in the x-axis. This assumption is checked later. Second, we assumed that the crosstalk from different channels is also additive. This must be verified by checking whether the crosstalk signal changes when two or more pixels have high count. For example, we should check whether the crosstalk in chA is doubled or not if chC and chD are hit by cosmic rays. In current data, such events are too few to make a conclusion. Third, we assume that the crosstalk does not affect the pixels in the same channel. It is difficult to check, since the local change of bias level from  $\Delta x=0$  cannot be distinguished from a change of the gain and the effect would be very small ( $\sim 10^{-4}$ ). The  $\Delta x=+2$  signal might be seen in the same channel, but we cannot distinguish the crosstalk signal from the original signal, as the intrinsic profile of the cosmic rays is unknown.

We checked the first assumption, the effects from different pixels are additive, using the crosstalk corrected images following the recipe. The profile after the correction is shown in Fig 12. As expected, the crosstalk is corrected well for single high count pixels, and most of the coefficients are consistent with no crosstalk ( $a = 0$ ). However, connected high count pixels show a significant sign that pixels at  $x=0$  in some combination have a significant signal. This means that the crosstalk phenomenon is not perfectly additive.

Recently, Nakaya et al. (2012) reported that preamp+SIG have a remnant signal of  $\sim 1$  ADU in following pixels in 4 channels after 50000 ADU signal in a channel. It corresponds to  $\sim 2 \times 10^{-5}$  of the coefficient at  $x = 1$  in our analysis. The different behavior of crosstalk after connected high value pixels may be a combined effect of the crosstalk and the remnant signal. Currently, it is difficult to investigate further because of the lack of sufficient data. Detailed investigation on this point will be possible when more data are available in future.

### 4.2. Application to the data

In the previous section, we get a recipe for the crosstalk correction for data with a negligible background. In this section, we will test the correction to the data with a background. We will apply the correction to two kinds of astronomical data. One is a narrowband image with a bright star. Such data has a low background sky level, and the effect of the crosstalk is apparent in a single image. The other is a deep field taken with a broadband filter. It is difficult to recognize the crosstalk in a single image, but the coadd enhances the S/N of the shadow. Then, we will estimate the effect of the crosstalk correction quantitatively.

#### 4.2.1. Narrowband images

For the first test, we used H $\alpha$ (N-A-L659) data of M83 of 720 seconds exposures, which were used in Koda et al. (2012). After flat-fielding, the background is typically 700 – 900 ADU, and rms is 20 – 40 ADU in a pixel. Saturated stars make blooming of  $\sim 60000$  ADU, and the shadow will be  $\sim 10$  ADU. An example is shown in the top pane of Fig 13. Though the crosstalk signal is  $0.2 - 0.5\sigma$  in a pixel, the corresponding shadow pattern is recognized in a single image, because the blooming pattern has a width of  $\sim 20$  pixels. The result of the correction is shown in the bottom pane of Fig 13. The apparent shadow is corrected by our recipe. Fig 14 is a surface brightness profile in 2 arc-sec apertures along x-axis of the two images. The shadow is corrected well.

### 4.2.2. Deep field

For the second test, we adopted a part of z-band(W-S-Z+) data of UV4a field. The exposure time is various between 180 sec to 720 sec. The median of the sky level is  $\sim 26000$  ADU. The position angle is the same for all the exposures, and the crosstalk shadows of the same parity overlap at the same position. We performed a standard reduction of Suprime-Cam. After the reduction, the shadow is not obvious in a single exposure, because of the high photon noise. However, it becomes apparent after the coadd of many exposures.

We picked up an example of the shadow as shown in Figure 15 top-left pane, and the coadd of the corrected data with our recipe is the top-right pane. Then, we divided the data into two subgroups according to the x-position of the dithering so that the celestial position shown in Figure 15 is affected by the crosstalk in the frames of one of the groups, and not in the frames of the other group. The numbers of the frames are 68(affected) and 86(not affected). The result of the coadd of each group is also shown in Figure 15 bottom-left and bottom-right. The surface brightness profile of 2 arcsec apertures along the x-axis is shown as Figure 16. It shows that the shadow at  $x=100$  is corrected well by our method (open circles), and the spatial profile of the coadd of the non-affected frames (filled triangles) is recovered.

## 5. SUMMARY

Using cosmic rays in dark frames, we evaluated the crosstalk in the new Suprime-Cam FDCCDs. The strength of the crosstalk is not affected by a change of the GAIN of the on-chip amps, which implies that the crosstalk occurs not inside the CCD but downstream from the output of the on-chip amp. The crosstalk effect is well approximated by a linear correlation. The coefficient seems to be correlated with the distance between the on-chip amplifiers in the CCD, which implies that the crosstalk occurs around on-chip amps. The coefficients are not significantly different among the 10 CCD CCDs. No crosstalk is detected among the different CCDs. We also find that the crosstalk appears not only the corresponding pixels but also at the next pixel but one. We present a recipe to remedy the crosstalk effect. The recipe is applied to the real data to show that it works well.

We thank the anonymous referee for suggestions which helped us to improve and clarify the manuscript. We appreciate Fumiaki Nakata for obtaining dark frames, Hidehiko Nakaya for the detailed information on readout system of Suprime-Cam, Yukiko Kamata and Hisanori Furusawa for the previous GAIN measurement of the CCDs. We appreciate Yutaka Komiyama and Satoshi Kawanomoto for suggestions and comments on the analysis. This work is based on archived data collected at the Subaru Telescope. The data are obtained from MASTARS, which is operated by the Subaru Telescope, and the SMOKA, which is operated by the Astronomy Data Center, National Astronomical Observatory of Japan.

## APPENDIX

### RELATIVE GAIN ESTIMATION

Data of Suprime-Cam has GAIN information of each channel in FITS header. The values should be  $g_1 \times g_2 \times g_3$ , where  $g_1$ ,  $g_2$ , and  $g_3$  are the gain of the analog-to-digital converter (ADC) in the SIG at each channel, the gain of the preamp of each CCD, and the gain of the on-chip amp at each channel, respectively.

The header values, however, are known to have large error<sup>10</sup>. The reason was that the preamp and the SIG used for the gain measurement were not the same as the currently used ones. Especially, a SIG board with one channel was used when the gain was measured. Therefore the GAIN values in the header represents  $k \times g_3$ , where  $k$  is an unknown coefficient of  $k = g_1(old) \times g_2(old)$ . As the gain of the preamp used for the measurement was  $g_2(old) = 4.19$ , while the typical gain of the preamps in the camera is  $\bar{g}_2 = 2.57$ , the factor was corrected in the FITS header values.

We can see the incorrect gain problem by multiplying flat images with the GAIN values in the FITS header at each channel. An example of CCD5 is shown in Fig 17 left. The flat pattern is the product of the quantum efficiency (QE) of each pixel, the throughput pattern of optics, and the inverse of the total gain. We can expect that the QE would be continuous at the channel boundary within a small variation. The optics pattern should be smooth. As there is a level gap between adjacent channels, it must be made by incorrect gain value ratios. Namely, it should reflect the variation of  $g_3$  among the channels in the same CCD.

In this study, we only require the ratio of the gains, since we expect that the crosstalk would be approximated by a linear relation as many other cameras follow. We therefore recalibrate the gain of each channel using dome flat so that the step between CCDs and channels to be minimal. As the gain of one channel (chA) of CCD9 is changed in 2010/10, we need to use a set before the change and after the change. We adopted 18 exposures of V, R, and I-band taken on 2010-06-10 for the former, and 38 exposures in V, R, and i-band taken between 2011-03-31 and 2011-04-04 for the latter. Each frame is divided by the median of the frame for normalization. Then, the median of the normalized frames is taken for each band and each CCD. This is a normal dome flat. We then extracted regions of 128 pixels wide across the channel boundary and binned by  $32 \times 32$  pixels. The left 2 binned pixels  $vL[1], vL[2]$  are in the left channel, and the other two pixels  $vR[3], vR[4]$  are in the right channel. From  $vL[1]$  and  $vL[2]$ ,  $vL[3]$  is estimated by linear extrapolation, and  $vR[2]$  is estimated from  $vR[3]$  and  $vR[4]$ . The ratio  $vR[3]/vL[3]$  and  $vR[2]/vL[2]$  reflect the ratio of the gains of the adjacent channels. The schematic figure is in Figure 18. As the y-pixels are 4177 in original flat,  $2 \times 130$  of the ratios are obtained. The median of the ratio gives the ratio of the gain of the adjacent channels in the CCD, and the error is estimated from median of the absolute deviation (MAD). We found that the ratio is the same within the error (typically  $\sim 0.05\%$ ) among different bands and in different epochs, except the chA of CCD9. This result supports that this method well extracts the relative gain information, as the flat pattern due to optics differs in different bands. We therefore took the median of the ratio of gains in all the bands. Except for the chA of CCD9, the two epochs are mixed to calculate the relative gain.

<sup>10</sup> [http://smoka.nao.ac.jp/help/help\\_SUPnewCCD.jsp](http://smoka.nao.ac.jp/help/help_SUPnewCCD.jsp)

We then estimated the ratio of the gain between neighboring CCDs. The similar method is adopted but we adopted a binning size of  $100 \times 100$  pixels, and ratios not only of x-neighbors but also of y-neighbors are calculated. The relative position and rotation of CCDs were estimated from night sky dithered exposures. We adopted the positions and the rotations as in Table 4. As the gain ratio information is redundant, we solved the overdetermined constraints by a singular value decomposition method.

The relative gain values are given in Table 2. The normalization is so that the chB of CCD5 to be unity, for the standard stars are often observed in the channel. The data reflect the relative values of  $g_1 \times g_2 \times g_3$ . The application of the new values is shown in Fig 17 right as an example, where the gaps disappear.

Dividing the re-calibrated relative gain ( $g_1 \times g_2 \times g_3$ ) by the GAIN values in the FITS header ( $k \times g_3$ ), we can obtain relative gain of SIG+preamps,  $g_1 \times g_2$ . The values are listed in Table 3. The normalization is also at the chB of CCD5. The change of the gain of chA of CCD9 in 2010/10 is thought to be the change of the on-chip amp and the gain of SIG+preamp remains the same.

#### REFERENCES

- Freyhammer, L. M., Andersen, M. I., Arentoft, T., Sterken, C., Nørregaard, P. 2001, *Experimental Astronomy*, 12, 147  
 Giavalisco, M. 2004a, STScI Instrument Science Report, ACS-ISR, 2004-12  
 Giavalisco, M. 2004b, STScI Instrument Science Report, ACS-ISR, 2004-13  
 Kamata, Y. et al. 2008, in Proc. SPIE 7021 "High Energy, Optical, and Infrared Detectors for Astronomy III." Ed. by Dorn, D.A., Holland, A.D., 70211S  
 Koda, J. et al. 2012, *ApJ*, 749, 20  
 Miyazaki, S., et al. 2002, *PASJ*, 54, 833  
 Nakaya, H., et al. 2008, in Proc. SPIE 7014 "Ground-based and Airborne Instrumentation for Astronomy II." Ed. by McLean, I. S., Casali, M. M., 70144X  
 Nakaya, H. 2012, *PASP*, 124, 485  
 Suchkov, A., Grogin, N., Sirianni, M., Cheng, E., Waczynski, A., Loose, M. 2010, STScI Instrument Science Report, ACS-ISR, 2010-10  
 Suchkov, A., Baggett, S. 2012, STScI Instrument Science Report, ACS-ISR, 2012-02

EXP-ID range	number of exposures	DATE-OBS	EXPTIME[sec]
SUPA010806{4,8,9}0,SUPA01082100	4	2009-03-27	200.0
SUPA01085760	1	2009-03-30	120.0
SUPA010886[2-7]0	6	2009-04-01	300.0
SUPA011221[5-7]0	3	2009-08-24	180.0
SUPA012194[0-2]0	3	2010-04-19	240.0
SUPA012921[2-9]0	8	2011-03-06	300.0
SUPA01331150-SUPA01331260	12	2011-06-03	300.0
total	37		

TABLE 1  
USED DARK EXPOSURES

DET-ID	chA	chB	chC	chD
0	1.050	1.063	1.083	1.069
1	1.070	1.138	1.217	1.212
2	0.995	1.019	1.038	0.947
3	1.022	1.040	1.042	1.154
4	1.006	1.128	1.085	1.033
5	1.015	1	0.972	1.082
6	1.190	0.987	0.984	1.034
7	0.971	1.059	1.067	0.981
8	1.011	1.252	1.276	1.172
9	0.994 <sup>a</sup> ,1.130 <sup>b</sup>	1.077	1.039	1.032

TABLE 2  
ESTIMATED TOTAL GAIN RELATIVE TO CHB OF CCD 5

<sup>a</sup>The gain is changed in 2010/10. The data is valid for the data before the change,

<sup>b</sup>The data is valid for the data after the change.

DET-ID	chA	chB	chC	chD
0	0.949	0.993	0.976	0.996
1	0.973	0.984	0.966	0.977
2	1.008	0.989	0.970	0.976
3	0.961	0.966	1.008	0.967
4	0.967	0.984	0.998	1.000
5	0.989	1	1.034	1.030
6	0.957	1.019	0.952	0.979
7	0.974	1.015	0.967	0.962
8	0.972	0.932	0.999	0.963
9	0.987	0.985	0.986	1.012

TABLE 3  
ESTIMATED GAIN OF SIG AND PREAMP RELATIVE TO CHB OF CCD 5

DET-ID	x[pix]	y[pix]	$\theta$ [rad]
0	3153.8	95.7	-0.00215
1	1047.7	95.9	-0.00033
2	-1066.5	98.5	-0.00015
3	3168.0	-4154.4	0.00264
4	1050.1	-4150.3	-0.00020
5	-1086.4	-4158.7	0.00014
6	-5310.5	96.7	-0.00055
7	-3187.3	97.7	-0.00003
8	-5346.6	-4177.5	0.00273
9	-3219.1	-4165.6	0.00040

TABLE 4  
RELATIVE POSITION AND ROTATION OF CCDS

pair	N <sub>data</sub>	<i>a</i>	<i>a<sub>min</sub></i>	<i>a<sub>max</sub></i>
gAB	9711	-1.42	-1.51	-1.33
gAC	9711	-1.48	-1.56	-1.40
gAD	8061	-1.67	-1.75	-1.59
gBC	1674	-0.62	-0.81	-0.44

TABLE 5

COEFFICIENTS OF BEST-FIT REGRESSION AND THEIR 95% CONFIDENCE INTERVALS ( $P(a_{min} < a < a_{max})=95\%$ ) IN  $v_1$  IN UNIT OF  $10^{-4}$

pair	N <sub>data</sub>	<i>a</i>	<i>a<sub>min</sub></i>	<i>a<sub>max</sub></i>
gAB	9905	-1.43	-1.52	-1.34
gAC	9905	-1.52	-1.60	-1.44
gAD	8231	-1.68	-1.76	-1.60
gBC	1674	-0.62	-0.80	-0.43

TABLE 6

SAME AS TABLE 5 BUT IN  $v_2$ .

$\Delta x$	gAB			gAC			gAD			gBC		
	<i>a</i>	<i>a<sub>min</sub></i>	<i>a<sub>max</sub></i>									
-1	0.12	-0.43	0.67	0.08	-0.42	0.57	0.01	-0.56	0.59	0.15	-0.65	0.96
0	-1.48	-1.83	<b>-1.13</b>	-1.62	-2.00	<b>-1.16</b>	-1.67	-2.00	<b>-1.28</b>	-0.77	-1.57	<b>-0.12</b>
1	0.02	-0.45	0.48	0.15	-0.38	0.67	-0.02	-0.60	0.57	0.06	-0.77	0.89
2	0.51	<b>0.13</b>	0.89	0.50	<b>0.15</b>	0.84	0.53	<b>0.18</b>	0.89	0.32	-0.37	1.00
3	0.13	-0.48	0.74	0.09	-0.46	0.63	0.07	-0.38	0.52	0.18	-0.53	0.90

TABLE 7

PART OF THE VALUES USED IN FIGURE 11 IN UNIT OF  $10^{-4}$ .

\*The values significantly different from 0, i.e.  $a_{max} < 0$  and  $a_{min} > 0$ , are in bold font.

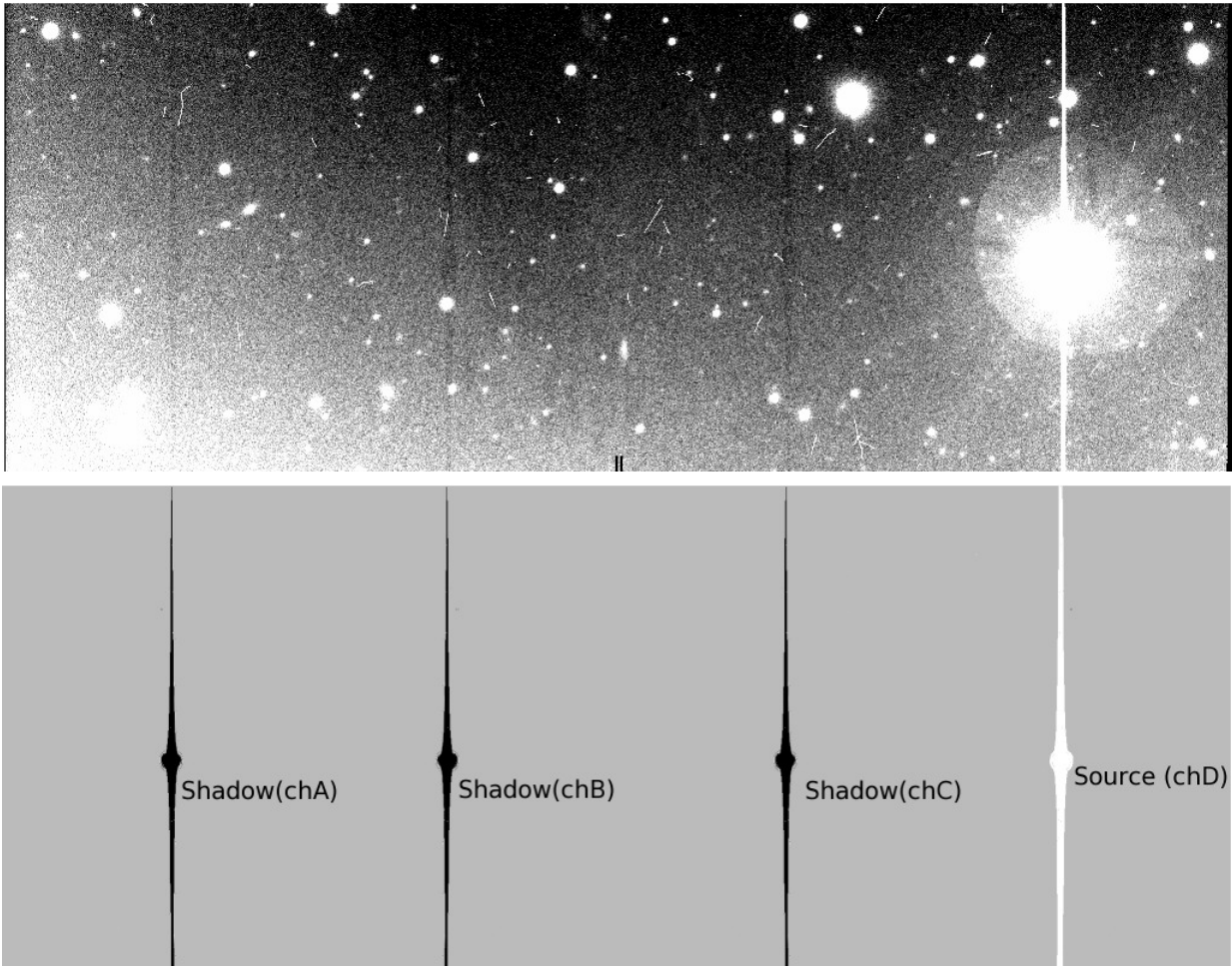


FIG. 1.— An example of a crosstalk. The bright star in chD makes shadows in chA, chB, and chC. (top) The image is a  $2048 \times 800$  pixels cutout from a single exposure of a bias-subtracted and flat-fielded image. (bottom) A schematic figure of the crosstalk source and its shadows of the top image.



FIG. 2.— A Schematic figures of the crosstalk effect after dithering. (left) When a bright object is observed in chA, shadows appears in chB, chC, and chD. (middle) If the telescope pointing changed toward top-left, the bright object moves toward bottom-right. Two of the shadows move toward bottom-left, while one in the chC moves toward the bottom-right. (right) As a result, the coadd of the two shots enhances the shadow in chC.

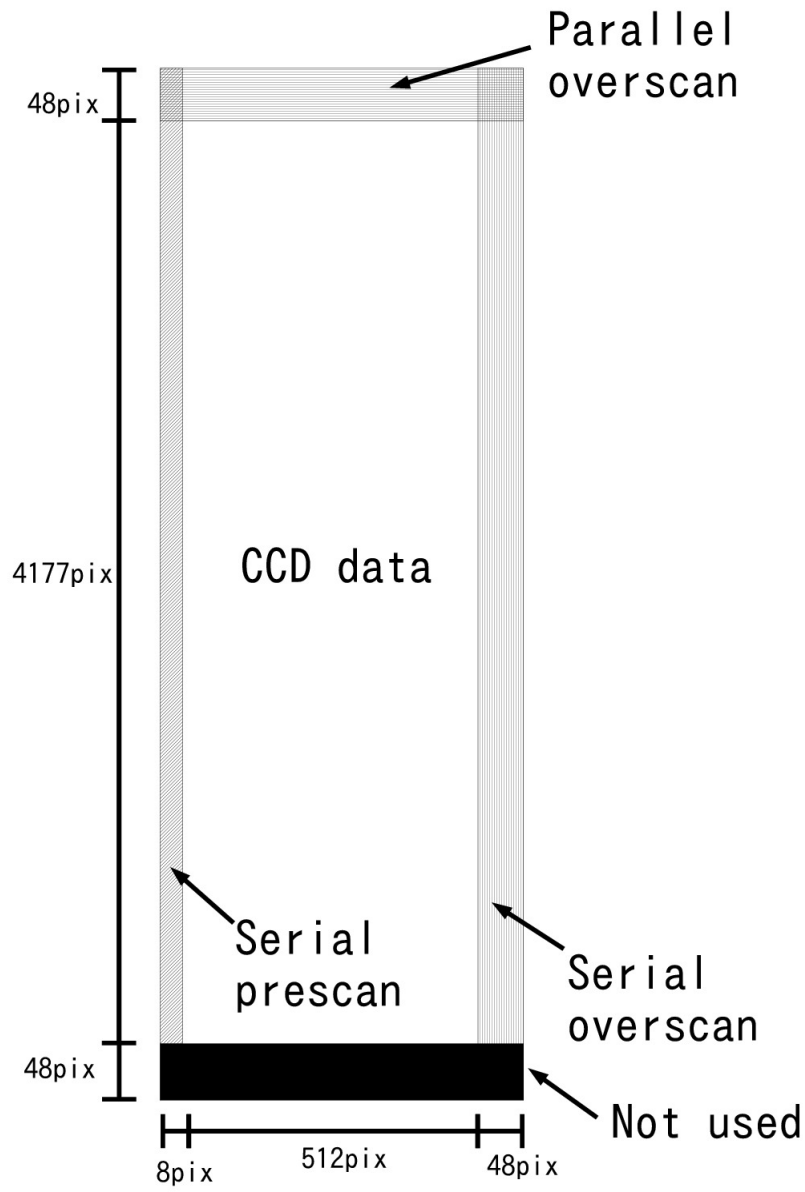


FIG. 3.— FITS data configuration of one channel of Suprime-Cam.

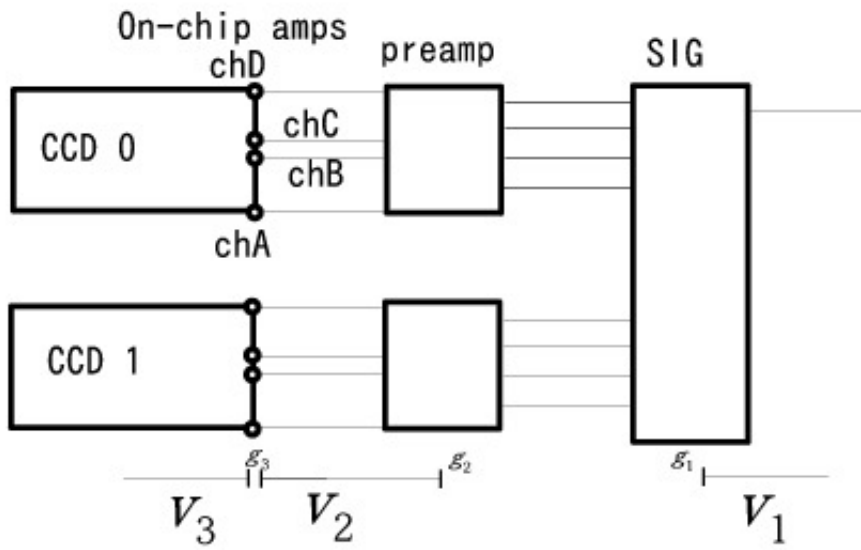


FIG. 4.— A schematic figure of the readout system of Suprime-Cam, and the names of signals used in this study

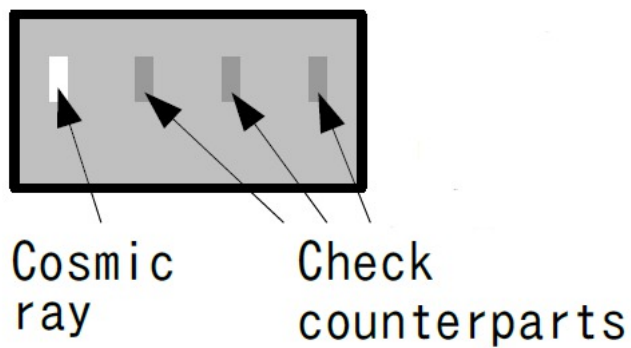


FIG. 5.— A schematic figure of the idea of our method to estimate the crosstalk effect.

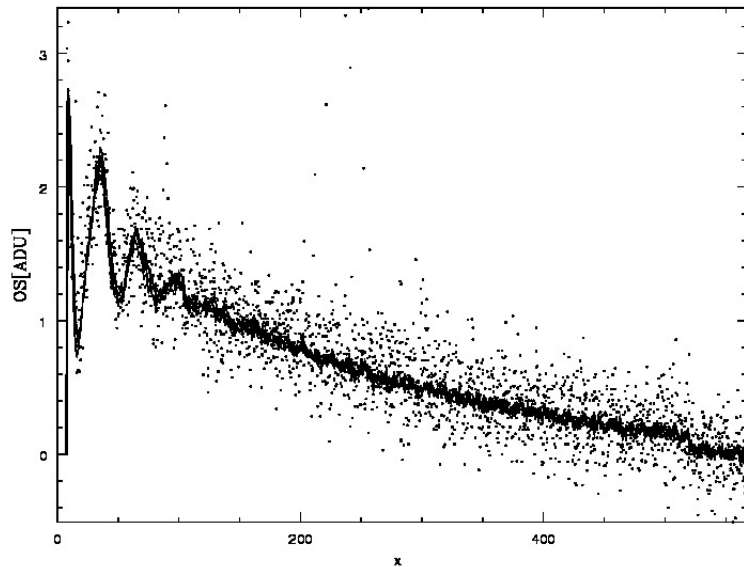


FIG. 6.— Example of Y-overscan. The dots are the parallel overscan of a frame(SUPA01181490) after the serial overscan subtraction. The data in 4 channels are plotted. The solid lines are the median of the parallel overscan function of 4 channels of 10 CCDs of 10 exposures. The prescan region (8 pixels at the left side) is discarded. The overscan region is 48 pixels at the right side.

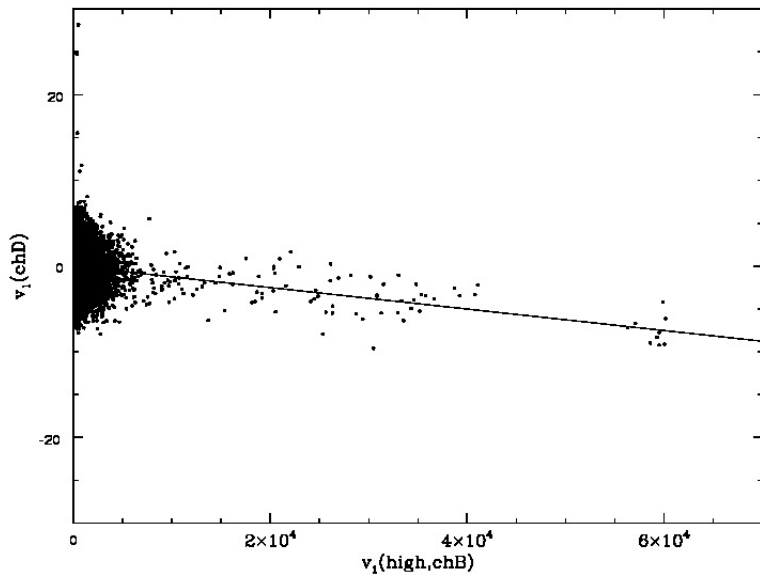


FIG. 7.— An example of crosstalk correlation. The high count pixel value at chB of CCD0 versus the pixel value at chD is plotted. All the exposures are used. The best-fit regression to the data are shown as the solid line.

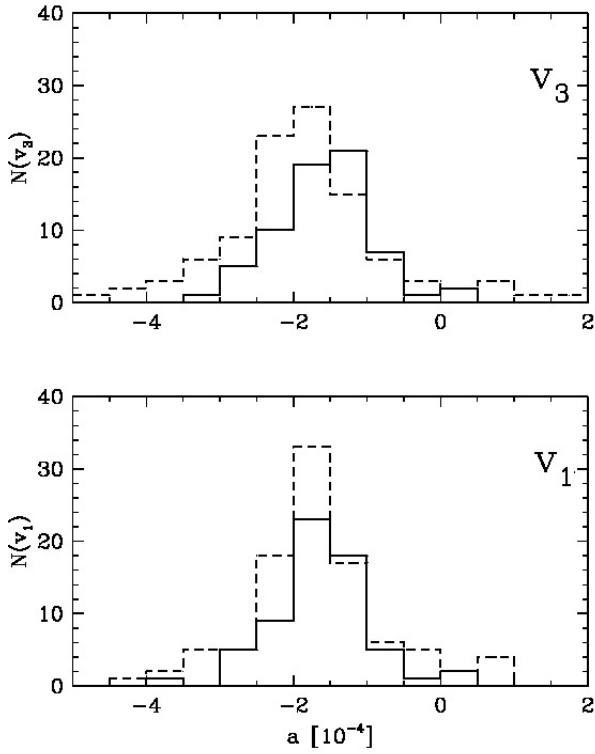


FIG. 8.— Histogram of  $a = v(\text{other})/v(\text{high})$  of CCD9 for high count pixel is chD, output is chA and  $v(\text{high}) > 15000$  data. The solid line is before the gain change and the broken one is after the change. The top panel is  $v_3$  and the bottom panel is  $v_1$ . The shape of the histogram of  $v_3$  varied with the change of the gain, while that of  $v_1$  was invariant.

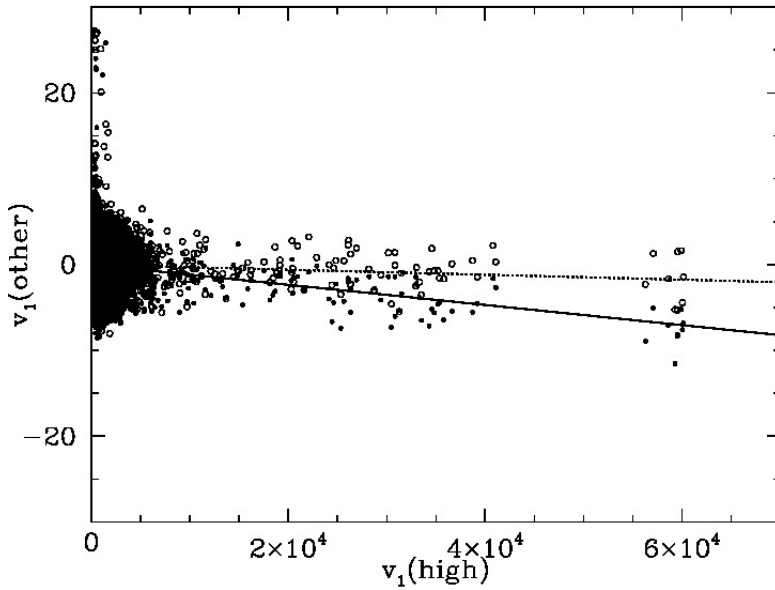


FIG. 9.— The high count pixel at  $v_1$  of chB vs  $v_1$  of chA (filled circles) and chC (open circles) of CCD0. The best-fit regression to the data are shown as the solid line(chA) and the dotted line(chC).

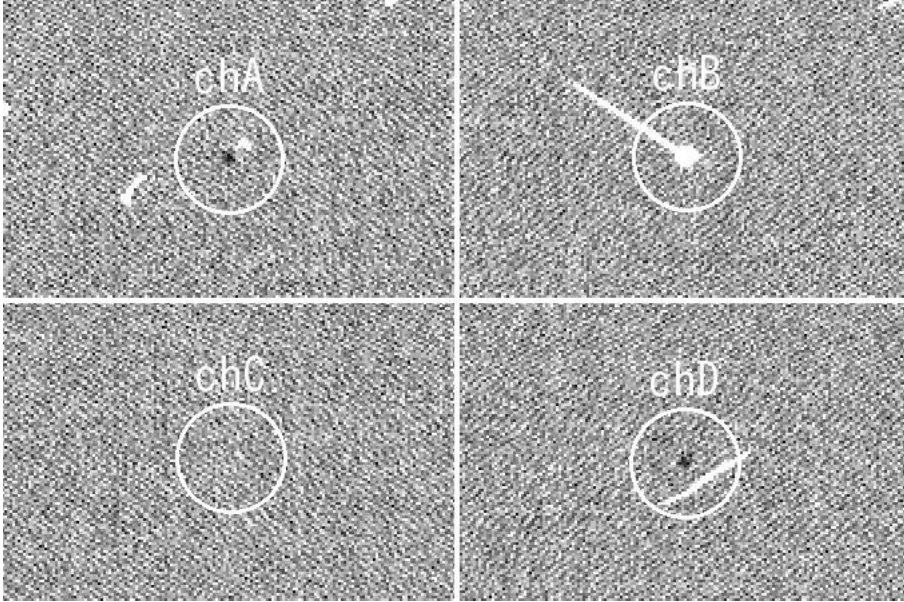


FIG. 10.— An example of different coefficients among channels. The images are cutouts of a dark frame. The color scale is the same for the four. A cosmic ray hit in chB, and the shadow appears in chA and chD. In chC, a shadow is not recognized around the corresponding pixel.

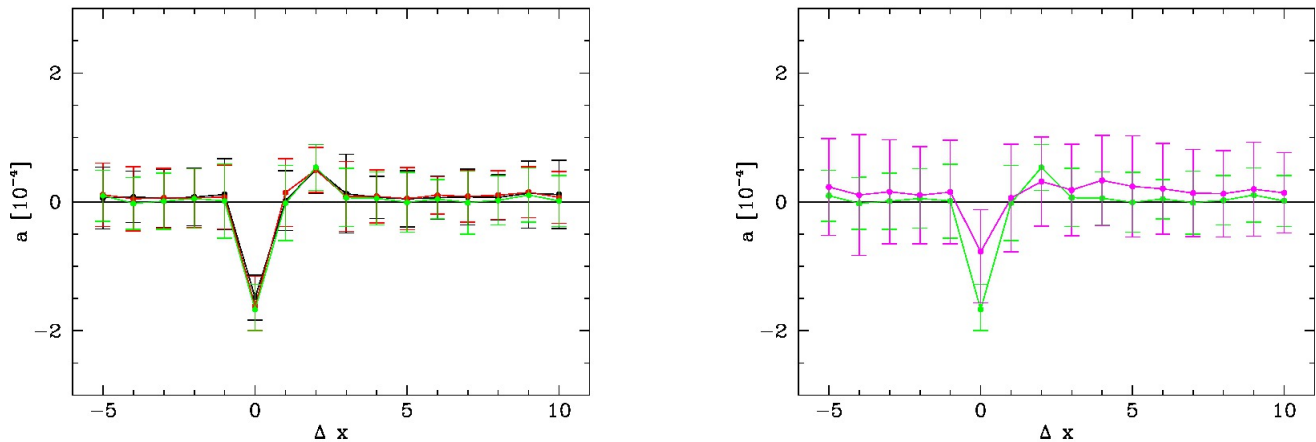


FIG. 11.— The crosstalk coefficients of adjacent pixels in  $v_2$ . Only the high count pixels which extend 1 pixel along the  $x$ -axis are used, and therefore the error is larger than the values in Table 5. The errorbars show 95% confidence intervals. At  $x=0$ , the high count pixel is read. The data read before the the high count pixel is read are shown in  $x<0$ , and those after the high count pixel is read are in  $x>0$ . (left) The profile of  $g_{AB}$ ,  $g_{AC}$ , and  $g_{AD}$  are plotted in black, red, and green, respectively. The coefficient is negative at  $x=0$ , which corresponds to the shadow. The three profiles are similar. (right) The profiles of  $g_{AD}$  and  $g_{BC}$  are plotted in green and magenta. The coefficient of  $g_{BC}$  is nearly zero.

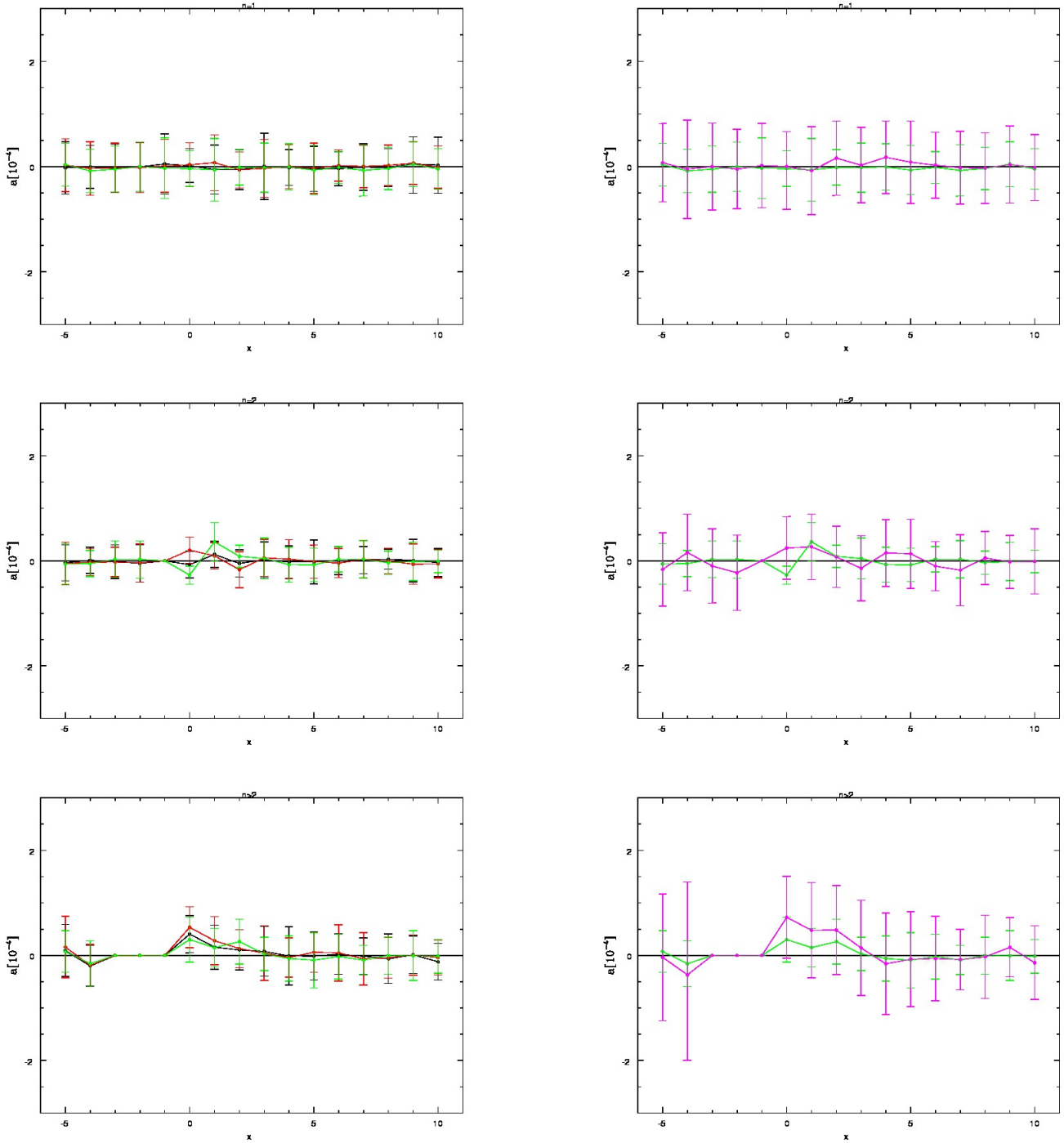


FIG. 12.— The crosstalk coefficients of adjacent pixels in  $v_2$  after our correction is applied. Top) The coefficients using high count pixels which extend 1 pixel along the x-axis. The color allocation is the same as Fig. 11. Middle) The coefficients using high count pixels which extend 2 pixels.  $x=0$  is the last one of the connected pixels. As  $x=-1$  is contaminated by the high count pixel, there is no data and coefficient is set to 0. Bottom) The coefficients using high count pixels which extend more than 2 pixels. The coefficients at  $x=-1$ , and  $x=-2$  is 0 because of no data.

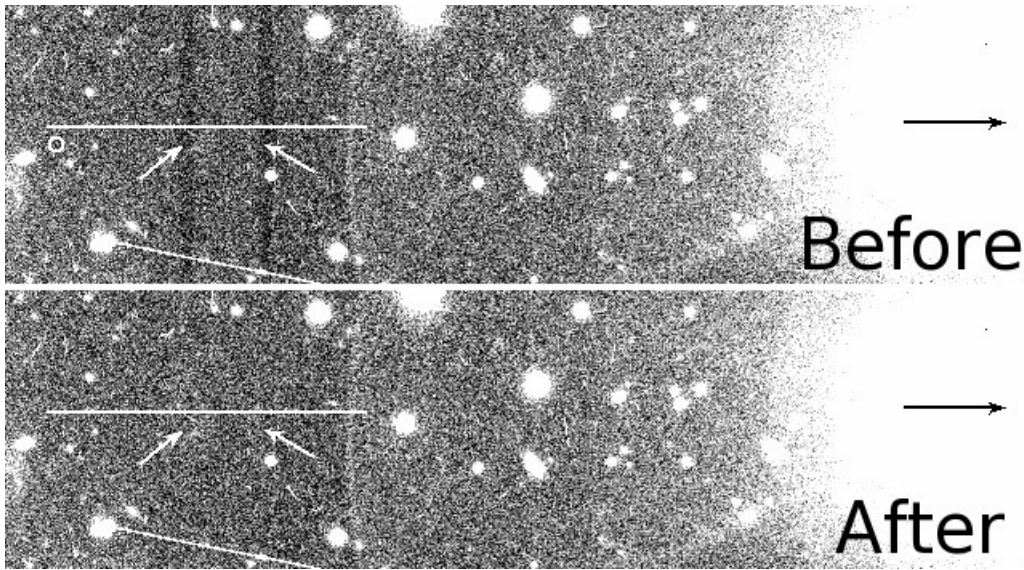


FIG. 13.— The effect of the correction for a narrowband image. The top panel is a cutout of a flat-fielded image and the bottom panel is that of a crosstalk-corrected and flat-fielded image. The black arrow shows a position of the saturated blooming in chD, and the white arrows show corresponding shadows in chB and chC by the crosstalk. The horizontal line shows the position of the profile shown in Fig 14, and the circle in the top panel indicates the 2 arcsec aperture size.

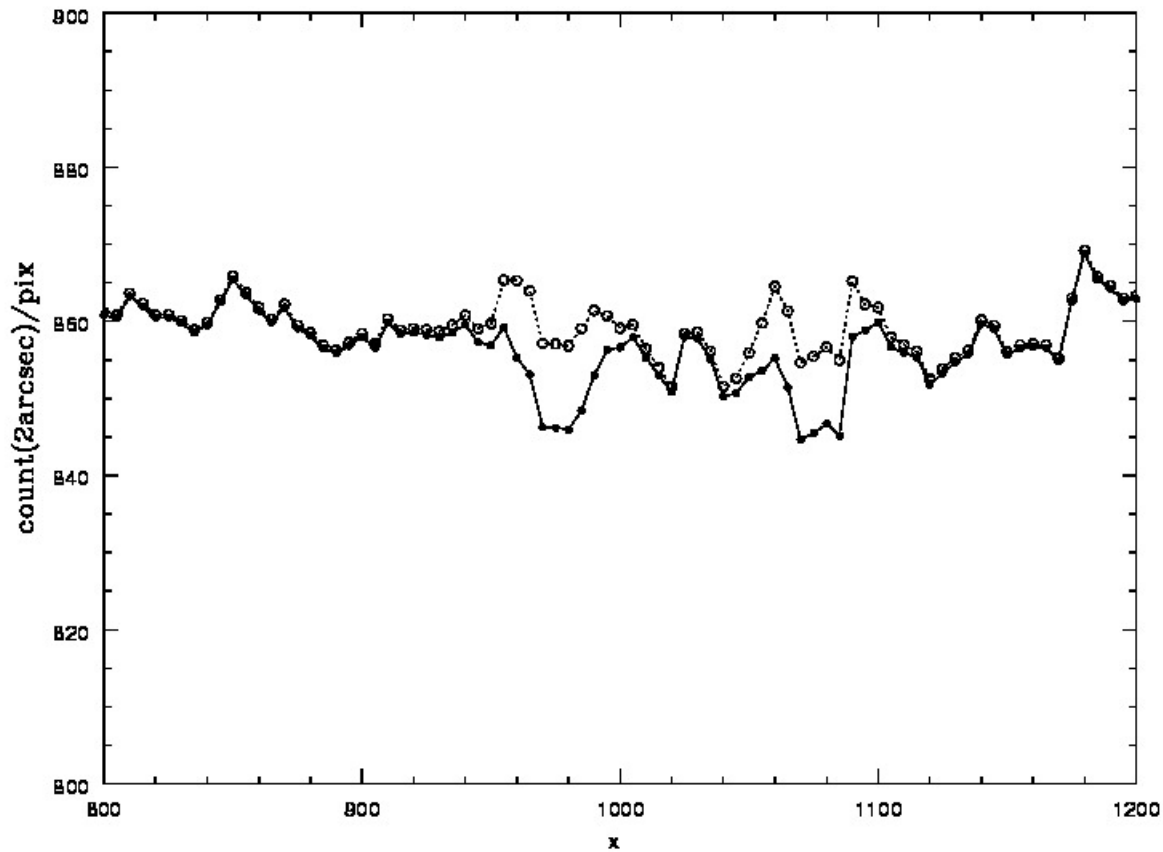


FIG. 14.— The surface brightness profiles of in 2 arcsec apertures along the x-axis. The images are Fig 13. The solid line with filled circles is the profile before the correction and the broken line with open circles is that after the correction. Around  $x=980$  and  $x=1080$ , the shadow is corrected.

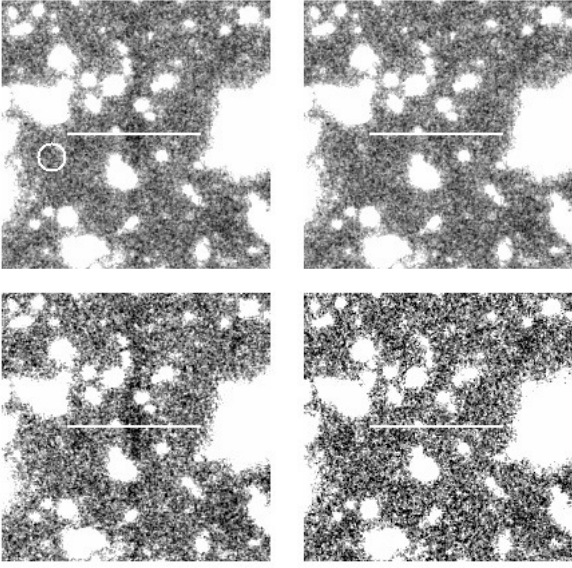


FIG. 15.— An example of the crosstalk effect in deep field data taken in broadband. The color scale is the same for the four panels. The horizontal line shows the position of the profile shown in Fig 16, and the circle in the top-left panel indicates the 2 arcsec aperture size. (top left) A cutout of a clipped mean coadd of the images without the crosstalk correction. A vertically elongated shadow is recognized. (top right) The same as the top-left but with the crosstalk correction. (bottom left) A clipped mean coadd of a subsample. The frames which would make the shadow at this position are used. (bottom right) The same as the bottom-left but those that would not create a shadow at this position are used.

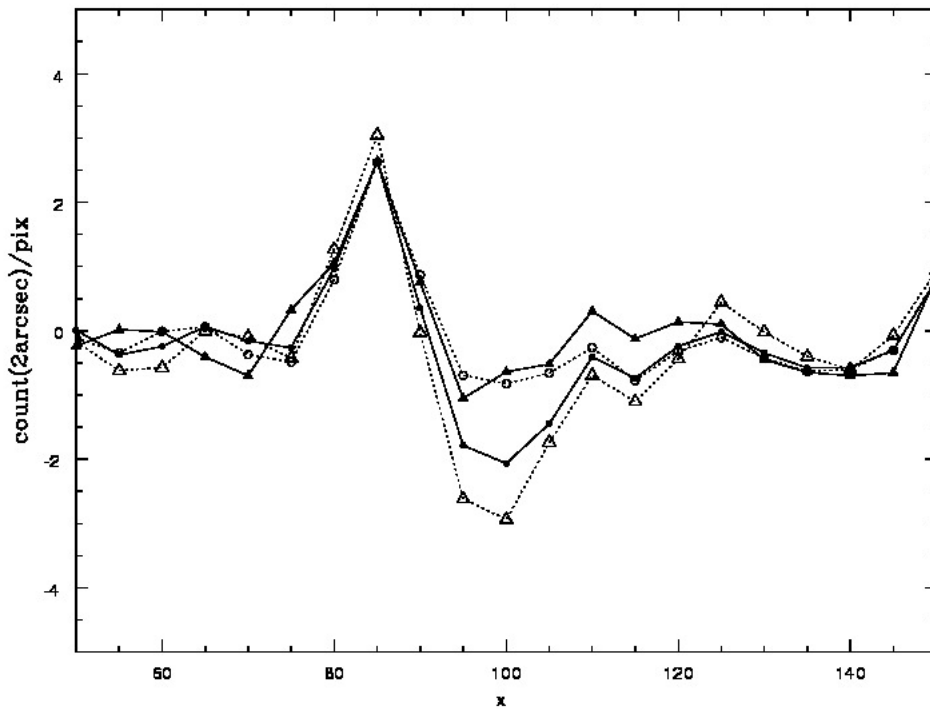


FIG. 16.— The surface brightness profiles of 2 arcsec apertures along the x-axis shown in Fig 15. The solid line with filled circles is before the correction, and the broken line with open circles is after the correction. The broken line with open triangles and the solid line with filled triangles represent the coadd of affected frames and that of unaffected frames respectively.

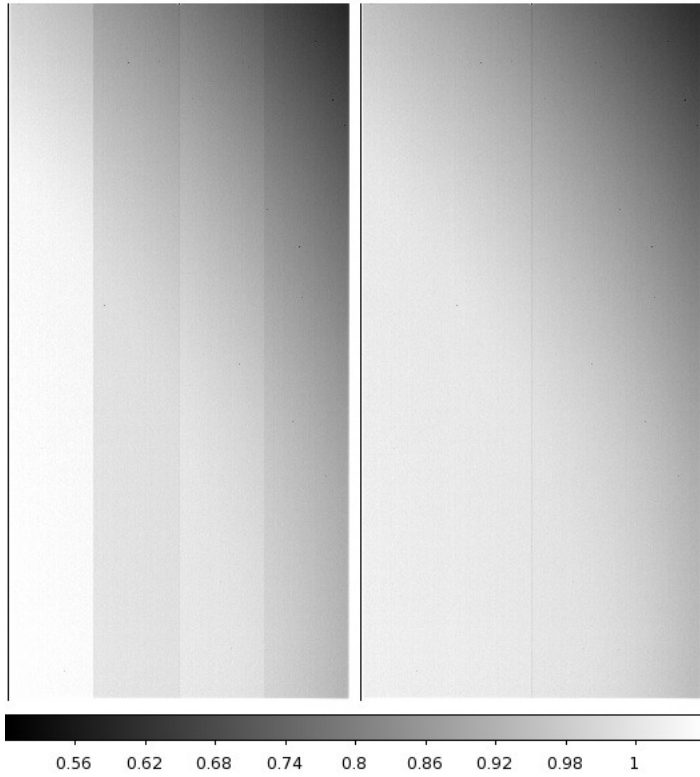


FIG. 17.— Improvement by the new gain data. A V-band domeflat of the CCD0 multiplied with gain at each channel. At left is the result with the original gain value, and at right is that with the new values (in Table 2). For comparison, the images are normalized so that the median of the image is unity, and the color scales of the two are the same.

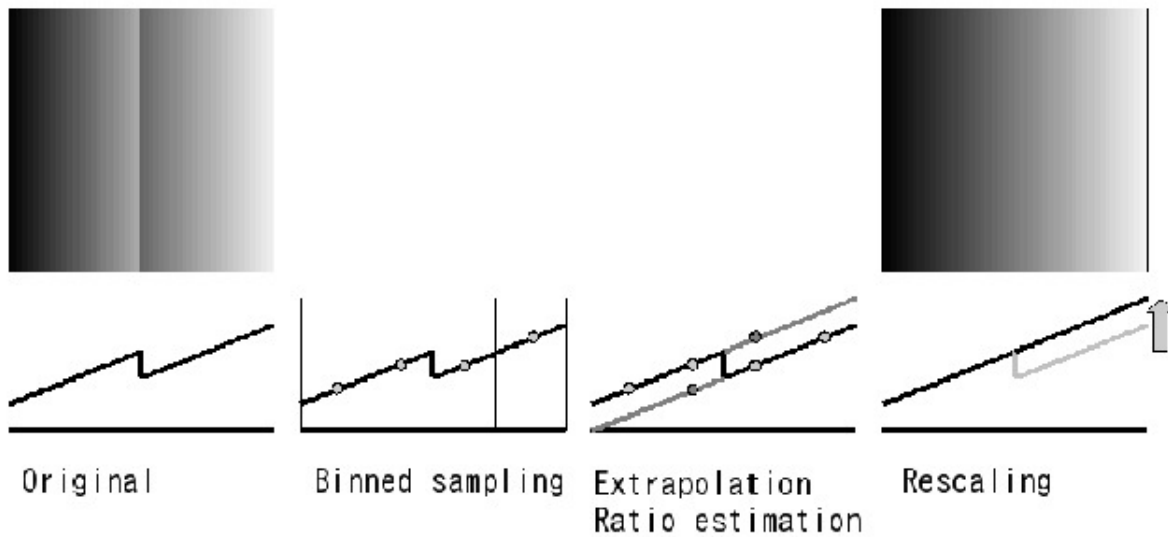


FIG. 18.— Schematic figure of the relative gain estimation.